Volume 48(1-4):13-17, 2004
Acta Biologica Szegediensis
http://www.sci.u-szeged.hu/ABS

ARTICLE

Ultralow-noise headstage and main amplifiers for extracellular spike recording

Dénes Budai*

Department of Biology, Juhász Gyula College, University of Szeged, Szeged, Hungary, and Kation Scientific Co., Minneapolis, MN, USA

ABSTRACT This methodological paper provides a detailed description of a novel ultralow-noise pre- and main-amplifier system designed for the extracellular recording of voltage spikes produced by neuronal action potentials. The main difficulties with extracellular recording are the unwanted electrical signals that lower the recording quality. They include destructive interferences by alternating electric or magnetic fields, in addition to thermal and other random noises resulting from the intrinsic properties of the substances from which the electrode and the electrical circuit are made. The preamplifier is placed in a specially built metal headstage probe. It is designed so that microelectrodes can be plugged directly into the probe, keeping the electrode and preamplifier in the closest possible proximity. Unique electrode holder adaptors at the same time make the probe for the electrode holder with the added benefit of extended electrical shielding. The main amplifier contains tuned circuit band pass filters optimized for metal and carbon fiber microelectrodes. Electromagnetic interference pickup is reduced by the enclosing tin-plated iron box and a built-in 50/60 Hz reject filter. In test experiments, an excellent signal-to-noise ratio and low-noise baseline recording were achieved. When carbon fiber microelectrodes were applied in the medulla of anesthetized rats, the total peak-to-peak noise level of the system was about 25 μV, *i.e.*, about 6 μV RMS, which is only a few μV higher than the theoretical random noise. It is concluded that, in combination with carbon fiber electrodes, the present amplifiers do not contribute significantly to the overall noise.
Acta Biol Szeged 48(1-4):13-17 (2004)

KEY WORDS

electromagnetic interference
random noise
grounding and shielding
band pass filtering
carbon fiber microelectrode
single-unit recording

Voltages generated by electric currents flowing in the tissue around the neurons during action potentials can be detected by means of microelectrodes as extracellular "spikes". Spike potentials recorded from the mammalian central nervous system have a duration of between 0.2 and 20 ms. The amplitudes of extracellular spikes are typically about 100 μV, although they may vary from the noise level (*vide infra*) of the electrode up to several mV, depending on the type of neuron and the quality of the recording system. The greatest advantage of extracellular recording is that the activity of neurons can be recorded without having to impale and consequently damage them. When multi-barreled microelectrode assemblies are used, extracellular recordings can easily be combined with microiontophoretic drug testing (Budai and Molnar 2001). For this and other reasons, most *in vivo* neuronal spike detection is carried out with extracellular recording. Signals picked up by an extracellular electrode are in the μV range and need to be amplified if they are to be processed in more conventional electronic devices such as oscilloscopes, analyzers or computers. The usual degree of amplitude amplification in extracellular amplifiers is around 10,000. The electrode must be connected to a specialized preamplifier (also known as a headstage) in order to work properly. The electrical properties of the headstage and main amplifiers set a limit to the smallness of signals that can be reliably measured.

The main difficulties with extracellular recording are the unwanted electrical signals or "noise" as it is popularly called. Noise in the present sense refers to unpredictable spontaneous voltage fluctuations, which appear as a thickening of the baseline when viewed on an oscilloscope at low sweep speed. An important distinction should be made, however, between the *interferences* (hum) from the mains power supply and the *random noise* that stems from the intrinsic properties of the substances from which the electrode and the electrical circuit are made (Purves 1981). Alternating electric fields give rise to capacitive coupling between the power lines and the microelectrode input circuit, and this coupling is responsible for a considerable proportion of the interference problems because of the high impedance of the microelectrode. Interference from alternating magnetic fields is another pernicious problem that can obscure microelectrode recordings. Thirdly, ground (earth) loops occur when ground leads are connected in such a way that a loop or cyclic path for current exists. A ground loop can act as a tuned circuit to pick up line frequency magnetic

Accepted Nov 16, 2004
*E-mail: kations@aol.com

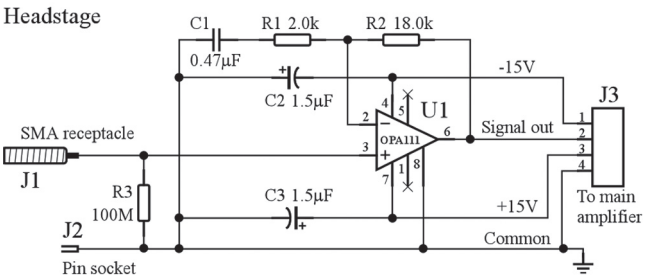

Figure 1. Schematic diagram of the headstage preamplifier. The low-noise, low bias current FET input operational amplifier (OPA111) is used as a non-inverting amplifier with a gain of 10.

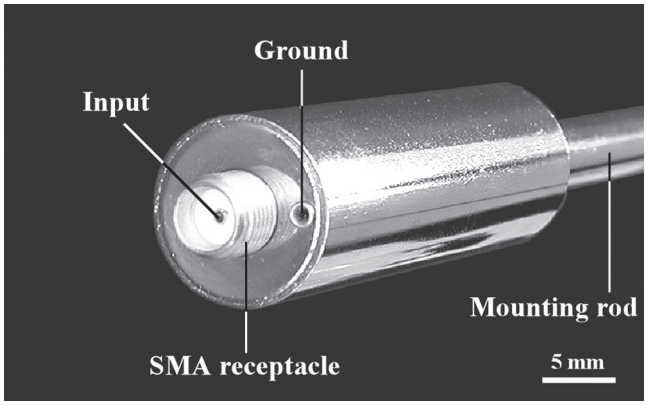

Figure 2. Physical layout of the headstage probe. The center receptacle of the SMA connector mates with the pin of the microelectrode, whereas its shell accommodates the electrode holder adaptors, as shown in Fig.3. The grounding pin is in galvanic contact with the metal parts of the headstage probe.

field radiation causing line hum interference. Transformers in line-powered equipment, microscope lamps and their associated wiring commonly cause both magnetic and electric field interference. Ground loops can form when a number of amplifiers are powered from a common direct current (DC) supply; they can be several meters in circumference if they go through ground leads to line-powered equipment.

There are four main sources of random noise in the input circuit for microelectrode recording: (1) the Johnson or thermal noise of the resistance of the microelectrode, (2) the voltage noise of the headstage preamplifier, (3) current noise of the preamplifier, and (4) "excess noise" in the microelectrode. The Johnson noise is due to the thermal motion of electrons, and sets a lower limit to the total noise. The voltage noise inherent in the preamplifier is the noise measured at the output when the input is grounded. The current noise comes from the miniature current that all operational amplifiers (op amps) have to draw in order to measure the voltage generated by the electrode. This current has a steady component (DC bias or leakage current), onto which random fluctuations are superimposed. The noise current flows through the parallel combination of electrode resistance and stray capacitance, producing a noise voltage. Microelectrodes display a noise component that is additional to their Johnson noise. This excess noise depends strongly on the voltage applied to the microelectrode, even though some excess noise is present in the absence of any applied voltage. The current noise is linearly dependent on the resistance of the electrode in contrast with the square root dependence exhibited by the Johnson noise. Both types of noise are band-limited by the low-pass filter consisting of the resistance of the electrode and the total input capacitance.

Not much can be done about the random noise, except to use electrodes with lower impedances at the frequencies necessary for spike recording. Careful selection of high-quality op amps and other parts is also of crucial importance in amplifier designs. The key specifications for the op amps are the bias current and voltage noise. Adherence to a few design rules, however, can greatly diminish the interferences resulting from alternating electric or magnetic fields and ground loops. Appropriate grounding and shielding in combination with a prudent physical layout of the experimental set-up eliminates the need for the fully enclosed Faraday cage of yesteryear. We described here a novel ultralow-noise headstage and main amplifier system for extracellular spike recording. This amplifier can be operated from batteries, totally independently from mains power. Its unique headstage probe design allows direct connection of the microelectrodes, further reducing destructive electromagnetic interferences and at the same time serves as an electrode holder.

Materials and Methods

Headstage amplifier

From an electronics viewpoint, our headstage or preamplifier is a classic non-inverting amplifier with gain (Horowitz and Winfield 1996; Fig. 1). In order to minimize interferences by alternating electromagnetic fields, microelectrodes can actually be plugged into the spark-plug type SMA receptacle of the headstage probe (J_1, Johnson Components, Part No. 142-0701-411), as shown in Figs 2 and 3. The miniature spring socket J_2 (AMP Inc., Part No. 50864) provides an input for the ground lead and mates with pin diameters ranging from 0.66 to 0.84 mm. The non-inverting input lead (pin 3) of the low-noise, low-bias current FET-input op amp, OPA111, is kept in mid-air and is directly soldered into the input pin of the SMA receptacle. The very short distance between the OPA111 and SMA connector and the PTFE (Teflon) insulation of the receptacle allows a leakage-free, low-noise connection between the microelectrode and the preamplifier. Resistors R_1 and R_2 should be of 1% tolerance or better and they provide a gain of 10, which is sufficient to bring the signal out of the amplifier noise region. The input shunt resistor R_3 should be used with

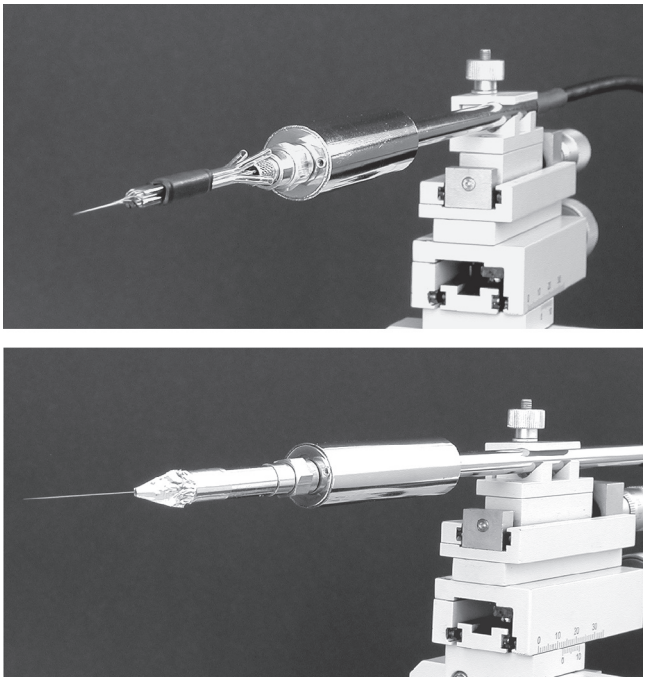

Figure 3. Use of the headstage probe in conjunction with multibarrel, carbon fiber-containing electrodes (upper panel) or with standard tungsten microelectrodes (lower panel). Note the adaptors for the two types of microelectrode. The metal electrode is held in place by copper foil with conductive adhesive, which also provides extended shielding for smooth recording.

tungsten or carbon fiber electrodes, but should be omitted for high-impedance electrodes. This resistor shunt removes DC and most low-frequency signals from the input (Millar 1992). Capacitor C_1 "rolls off" the gain to unity at low frequencies or DC to stop the amplifier saturating if DC potentials exist at the electrode (Millar and Barnett 1994). Small tantalum capacitors C_2 and C_3 bypass the ±15 V power supply leads to 0 V to prevent oscillation. The metal can of the OPA111 should be grounded (pin 8) for additional shielding of the front-end op amp.

The physical layout of the headstage probe is shown in Fig. 2 and 3. The entire circuitry is placed in a 14 mm x 50 mm (diameter x length) nickel-plated cylindrical brass container for added shielding from electromagnetic interference. Microelectrodes can be inserted directly into the center pin of the SMA connector fixed in the front-end of the probe (Fig. 2). The center pin is embedded in a PTFE insulator, whereas the grounding receptacle is in galvanic contact with the metal parts of the headstage probe. Two types of electrode holder adaptors (modified SMA plugs) can be screwed onto the SMA connector, making the headstage at the same time for an electrode holder. One is used to attach glass-insulated single or multibarrel carbon fiber electrodes (Armstrong-James and Millar 1979; Millar and Williams 1988; Budai and Molnar, 2001; Millar and Pelling 2001), as shown in Fig. 3. The other type of adaptor is used to accommodate small-diameter metal electrodes. To configure this type of electrode holder, the connector pin of the electrode is inserted first into the front of the adaptor and pulled through it so that it protrudes somewhat from the back-end of the adaptor. This is done on a flat surface before the adaptor is screwed onto the SMA connector. A small pair of tweezers is used to grasp the pin of the electrode and insert it into the input socket of the probe. The adaptor is then screwed onto the probe gently by hand. Next, an about 2.5 cm-long strip of copper foil with conductive adhesive tape (3M, Part No. 1181) is rolled cylindrically so that one-third of the 25 mm width of the tape is around

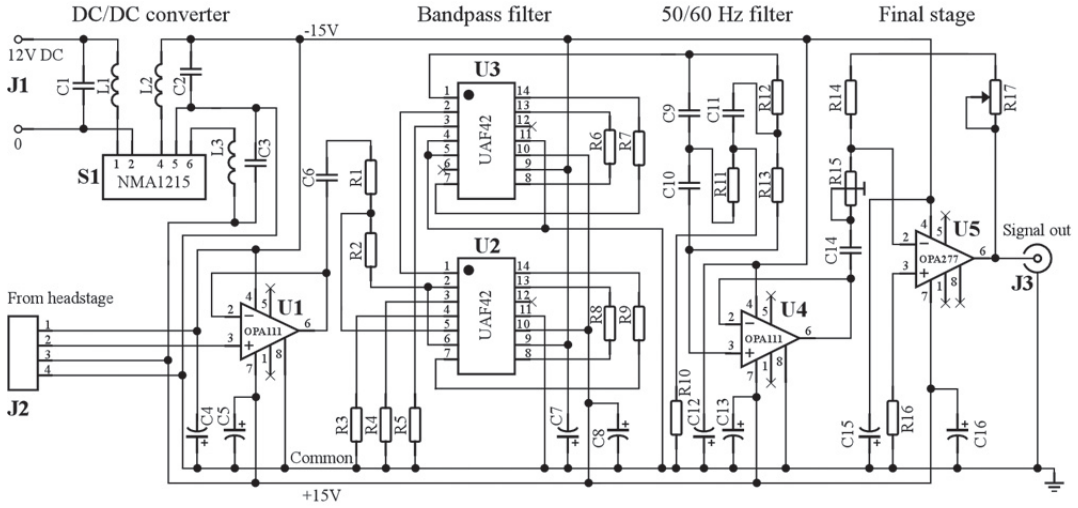

Figure 4. Schematic diagram of the main amplifier, showing details of the DC-DC converter, signal input buffer, band pass and notch filtering, as well as the final gain stages. See Table 1 for specific part values.

the front-end of the adapter and two-thirds of it is around the shank of the electrode itself. Finally, the front-end of the tape is flattened with the thumb and forefinger and the excessive parts of the foil are cut off. The copper foil has a twofold purpose: it holds the electrode in place and it provides an extended shielding for smoother recording. The end-result of this procedure is illustrated in Fig. 3. The headstage probe can be securely fixed in most micromanipulators via its 6.4 mm x 105 mm (diameter x length) mounting rod, which also serves as a cable guide. The headstage probe is connected to the main unit by a 1.5-m-long, well-shielded, high-flex cable (Belden, Part No. A3308) through the use of a four-pole, screw-on connector (Hirose, Part No. SR30-10PE-4P) placed on the free end of the cable.

Main amplifier

Miniature DC-DC converters allow a very space-saving solution to make dual ±15 V rail supplies available on board. The S_1 NMA1215S in the main amplifier can utilize almost any 12 V DC source for input, including good-quality external AC-DC converters or batteries. It is a fully encapsulated DC-DC converter, with the added benefit of galvanic isolation to reduce switching noise. The DC input and outputs are smoothed by LC filters (L_1-L_3, C_1-C_3; Fig. 4). Specific values for each part reference are given in Table 1.

Table 1. List of materials for the main amplifier

Item	Quantity	Reference	Value	Manufacturer
1	3	C1, C2, C3	1.0 µF	Panasonic
2	8	C4, C5, C7, C8, C12, C13, C15, C16	2.2 µF Ta	Panasonic
3	1	C6	0.83 µF	Panasonic
4	1	C14	3.3 µF	Panasonic
5	2	C9, C10	500 pF	Panasonic
6	1	C11	1000 pF	Panasonic
7	1	J1 DC power jack	163-1021	Kobiconn
8	1	J2 Four-pin receptacle	SR30-10R-4S	Hirose
9	1	J3 BNC jack	30-10-RFX	Amphenol
10	1	L1	47 µH	J.W. Miller
11	2	L2, L3	330 µH	J.W. Miller
12	1	R1	2 kΩ	Yageo
13	1	R2	100 kΩ	Yageo
14	2	R3, R16	10 kΩ	Yageo
15	2	R4, R5	22 kΩ	Yageo
16	2	R6, R7	68 kΩ	Yageo
17	2	R8, R9	33 kΩ	Yageo
18	1	R10	10 Ω	Yageo
19	1	R11	3.16 MΩ	Phicomp
20	2	R12, R13	6.37 MΩ	Phicomp
21	1	R14	100 Ω	Yageo
22	1	R15 Trimmer potentiometer	2 kΩ	Bourns
23	1	R17 Potentiometer	50 kΩ	Precision Electronic
24	1	S1 DC-DC converter	NMA1215S	C&D Technologies
25	1	U1	OPA111AM	TI/Burr-Brown
26	1	U4	OPA111BM	TI/Burr-Brown
27	2	U2, U3	UAF42AP	TI/Burr-Brown
28	1	U5	OPA277AP	TI/Burr-Brown

*Values for 50 Hz. For 60 Hz, use 2.67 MΩ and 5.34 MΩ, respectively

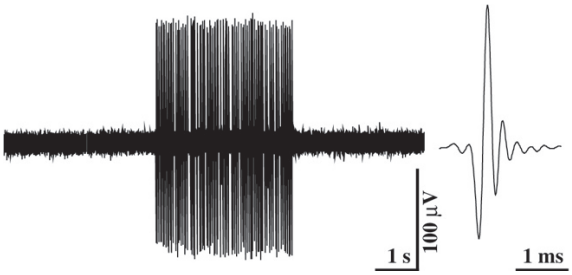

Figure 5. Single-unit recording from a medullary neuron in an anesthetized rat. Spikes were evoked by peripheral stimulation. Note the excellent signal-to-noise ratio and the low-noise baseline recording.

The U_1 op amp buffers signals arriving from the headstage preamplifier and its output are AC-coupled (C_6) to the band pass filter stage (Fig. 4). Before filtering, the signal is amplified by the uncommitted op amp of the U_2 UAF42 universal active filter(UAF42 Datasheet, 1998) and resistors R_1 and R_2. A tuned circuit band pass filter for the spike bandwidth (approximately 300 Hz to 8000 Hz) is constructed, using two UAF42 active filters (U_2 and U_3) and the network of resistors R_3-R_9 (Molina and Stitt 1993). To reduce electromagnetic interference from the mains line power, an additional 50/60 Hz reject (notch) filter is included. This is comprised of an OPA111BM op amp (U_4), resistors R_{10}-R_{13} and capacitors C_9-C_{11}. Resistors R_{11}-R_{13} define the reject frequency; different resistor values are used for 50 Hz and 60 Hz, as specified in Table 1 (OPA111 Datasheet, 1995). The notch filter stage is AC-coupled (C_{14}) to the final, variable-gain stage that consists of the op amp U_5 and resistors R_{14}, R_{15} and R_{17}. Potentiometer R_{17} is placed on the front panel to adjust the required gain during an experiment, while trimmer potentiometer R_{15} is for calibration of the overall gain in the whole system.

The layout of the circuit is not critical except for the wiring at the non-inverting input of U_1. This wiring is performed with stiff wire in mid-air. The entire circuit is placed in a tin-plated iron box in order to minimize electromagnetic interference. With the part values listed in Table 1, the main amplifier produces a max signal gain of about 1,000. During application of a 10 mV peak-to-peak sine wave signal with a frequency of 1 kHz at the input connector J_2, the trimmer R_{15} can complete fine calibration of the main amplifier. The input calibrating, signal together with the output amplified signal, should be adjusted and observed by using a calibrated two-channel oscilloscope. The signal will already have been amplified by 10 in the headstage amplifier, and thus the overall gain in the whole system is 10,000. Resistors R_1, R_2 and/or R_{14}, R_{15} or R_{17} should be replaced with the required values if a different system gain is necessary. The actual appearance of the main amplifier has been published on the Internet (Budai 2004b).

Extracellular recording *in vivo*

Sprague-Dawley rats (300-400 g) of either sex were initially anesthetized with chloral hydrate (40 mg/100 g, i.p.; supplemental doses as required). All procedures relating to animal handling and surgery followed the protocol for animal care approved by the Hungarian Health Committee and the international guidelines (EC Directives, 86/609/EEC). Experimental details have been published previously (Budai and Molnar 2001). In brief, single-unit recordings were made from neurons of the medulla located between the planes from 11 mm to 12 mm behind the bregma (Paxinos and Watson, 1998) using the headstage and main amplifiers described above. Spike potentials were recorded with a four-barreled micropipet assembly in which one of the barrels contained a 7-µm carbon fiber creating a low-impedance (0.4-0.8 MΩ at 1 kHz) recording electrode (Budai and Molnar 2001) as shown in Fig. 3. The experimental data collection was automated by means of a multifunction instrument control and data acquisition board (PC-1200, National Instruments, Austin, TX) programmed in LabView (National Instruments, Austin, TX). The LabView-based data acquisition and instrument control software was developed in-house; it has been published in part elsewhere (Budai 1994, 2004a). Analog signals were sampled and digitized at 50 kHz by the data acquisition card, and oscilloscope trace-like recordings were taken from all neurons.

Results and Discussion

If the measured noise voltages are squared and the mean square is computed, the fluctuations of both signs contribute positively. The square root of this mean (RMS) is the usual way of expressing the magnitude of noise voltages. The RMS of the Johnson noise is $(4kTR\Delta f)^{1/2}$, where k is the Boltzmann constant (1.38×10^{-23} JK^{-1}), T is the absolute temperature in Kelvin, R is the resistance of the microelectrode in ohm, and Δf is the noise bandwidth in Hz. If Δf is 5 KHz, this formula gives 5.6 µV RMS for thermal noise in the case of carbon fiber electrodes with a resistance of 0.4 MΩ, when the temperature is 20ºC= 293ºK. When the input of the described headstage amplifier was grounded, the voltage noise in the whole system was no more than 1 µV RMS. On the use of four-barrel, carbon-fiber containing assemblies of borosilicate glass micropipets (Fig. 3) in the medulla of anesthetized rats, the total peak-to-peak noise levels increased to about 25 µV, *i.e.,* to about 6 µV RMS. This means that our headstage and main amplifier system is very close, in terms of noise performance, to its theoretical lower limit and does not contribute significantly to the overall noise. We conclude that our preamplifier, in combination with carbon fiber electrodes, performs equally well or rather better than those described previously (Millar and Williams 1988; Millar and Barnett 1994).

Figure 5 illustrates a low-noise recording from a medullary neuron with a four-barrel carbon fiber microelectrode. Spike responses were evoked by peripheral somatosensory stimulation applied to the tail. Noteworthy features include the excellent signal-to-noise (spike-to-baseline) ratio and the very low-noise baseline recording. At times, tungsten electrodes shielded by our unique adaptor/holder (Fig. 3) produced even lower-noise recordings (data not shown). The copper foil shielding can be extended by a brushable shield through the use of silver paint or colloidal silver (Sachs 1985). By this means, the shielding could be extended very close to the tip of the microelectrode and, could possibly, further reduce interferences from electric fields as the impedance of metal or carbon fiber electrodes is largely capacitive (Robinson 1968) and only the real component of the complex impedance of the electrode contributes to thermal noise (Millar and Barnett 1994).

Acknowledgment

This work was funded by Kation Scientific Co., Minneapolis, MN 55105, USA.

References

Armstrong-James M, Millar J (1979) Carbon fibre microelectrodes. J Neurosci Methods 1:279-287.

Budai D (1994) A computer-controlled system for post-stimulus time histogram and wind-up studies. J Neurosci Methods 51:205-211.

Budai D (2004a) Software. http://www.kationscientific.com/iontophoresis/ratemeter.html

Budai D (2004b) Action potential recording. http://www.kationscientific.com/iontophoresis/spikeamps.html

Budai D, Molnar Z (2001) Novel carbon fiber microelectrodes for extracellular electrophysiology. Acta Biol Szegediensis 45:65-73.

Horowitz P, Winfield H (1996) The art of electronics. New York: Cambridge University Press.

Millar J (1992) Extracellular single and multiple unit recording with microelectrodes. In: Monitoring neuronal activity: a practical approach (Stamford JA, ed), pp 1-27. Oxford: Oxfor University Press.

Millar J, Williams GV (1988) Ultra low-noise silver-plated carbon fibre microelectrodes. J Neurosci Methods 25:59-62.

Millar J, Barnett TG (1994) A low-noise optically isolated preamplifier for use with extracellular microelectrodes. J Neurosci Methods 51:119-122.

Millar J, Pelling CW (2001) Improved methods for construction of carbon fibre electrodes for extracellular spike recording. J Neurosci Methods 110:1-8.

Molina J, Stitt RM (1993) Filter design program for the UAF42 universal active filter. http://focus.ti.com/lit/an/sbfa002/sbfa002.pdf

OPA111 Datasheet (1995) Burr-Brown Division of Texas Instruments. http://focus.ti.com/lit/ds/symlink/opa111.pdf

Paxinos G, Watson C (1998) The rat brain in stereotaxic coordinates, 4th Edition. New York, NY: Academic Press.

Purves RD (1981) Microelectrode methods for intracellular recording and iontophoresis. London: Academic Press.

Robinson DA (1968) The electrical properties of metal microelectrodes. Proc IEEE 56:1065-1071.

Sachs F (1985) Microelectrode shielding. In: Voltage and patch clamping with microelectrodes (Smith TG, Lecar H, Redman SJ, Gage PW, eds), pp 25-45. Baltimore: Waverley Press.

UAF42 Datasheet (1998) Burr-Brown Division of Texas Instruments.